NEW RESONANCES AT BELLE*

Jolanta Brodzicka

H. Niewodniczański Institute of Nuclear Physics
Polish Academy of Sciences
Radzikowskiego 152, 31-342 Kraków, Poland

(Received December 13, 2004)

I summarise Belle results on new discoveries in meson spectroscopy. Two broad D^{**} mesons that are P-wave excitations of the $c\bar{u}$ system as well as two narrow D_{sJ} states interpreted as orbitally excited P-wave $c\bar{s}$ states have been observed. Moreover, the $X(3872)$ charmonium-like state has been discovered. Mass of this state being very near $M_D + M_{D^\star}$ mass threshold could indicate molecular nature of newly observed state.

PACS numbers: 14.40.Gx, 12.39.Mk, 13.20.He

1. Introduction

Many interesting and unexpected discoveries in meson spectroscopy have been recently reported. I will discuss the discoveries made in B-factories experiments. B-factories are very rich and clean source not only B mesons but also charmed particles thus giving an excellent opportunity to search for new states with charm quark content.

The BaBar experiment has claimed the discovery of the narrow $D_s\pi^0$ resonance at 2317 MeV produced in a $e^+e^- \to c\bar{c}$ continuum process [1]. The CLEO collaboration has observed a nearby narrow $D_s^\star\pi^0$ state [2] at 2463 MeV, and the Belle experiment confirmed the existence of two new mesons, by observing their production in a continuum and B meson decays [3, 4].

The observed decay channels indicate $c\bar{s}$ quark composition of newly found mesons. They are interpreted as orbitally excited P-wave $c\bar{s}$ states, even though these assignments contradict the potential model predictions [5, 6]. The mass difference between the two observed states is consistent with the expected hyperfine splitting of the P-wave D_s meson doublet with

* Presented at the XLIV Cracow School of Theoretical Physics, Zakopane, Poland, May 28–June 6, 2004.

$j_s = 1/2$. However, the observed masses and widths are considerably lower than those predicted by the potential model. Their decays to the $D^\star K$ modes are not allowed kinematically. The D_{sJ} states are observed in isospin-violating decays to $D_s^{(\star)}\pi^0$ and are very narrow. Because of these discrepancies with the potential model predictions, more exotic assignments have been also proposed for the new states such as DK molecular states, multiquark states or mixtures of P-wave $c\bar{s}$ meson and 4-quark $c\bar{s}q\bar{q}$ state [7, 8]; chiral partners of D_s and $D_s^\star$, pseudoscalar and vector states [9,10]. The measurements of their properties and quantum numbers are essential to determine the nature of the newly found states.

Two new D^{**} states that are P-wave excitations of the $c\bar{u}$ system have been observed by Belle in $B^- \to D^{(\star)+}\pi^-\pi^-$ three-body decays [11]. In a coherent amplitude Dalitz plot analysis broad resonances have been found: a scalar $D_0^\star$ in $D^+\pi^-\pi^-$ final state, and a pseudovector D_1' in $D^{(\star)+}\pi^-\pi^-$. Masses and widths of newly found D^{**} states are consistent with the potential models predictions.

Another interesting discovery made by the Belle concerns the $X(3872)$: a narrow charmonium-like state produced in exclusive decay process $B^\pm \to K^\pm J/\psi\pi^+\pi^-$ [12]. Mass of this state being very near $M_D + M_{D^\star}$ mass threshold could indicate molecular nature of newly observed state [13]. Other interpretations include $c\bar{c}g$ "hybrid charmonium" [14] or ordinary charmonium state [5, 6, 15].

2. The Belle experiment

The Belle experiment, devoted to CP violation studies in B meson decays, is performed at the KEKB asymmetric energy e^+e^- collider. The KEKB collider operates at the centre of mass energy $\sqrt{s} = 10.58$ GeV equal to the $\Upsilon(4S)$ mass. Its peak luminosity exceeded 1.3×10^{34} cm^{-2}s^{-1}. About 274×10^6 $B\bar{B}$ pairs and 350×10^6 $c\bar{c}$ events have been collected with the Belle detector until summer 2004.

The Belle detector is a general purpose magnetic spectrometer equipped with a 1.5 T superconducting solenoid magnet. Charged tracks are reconstructed in a 50 layer Central Drift Chamber and in three layers of double sided silicon strip detectors of the Silicon Vertex Detector. Photons and electrons are identified using the CsI(Tl) Electromagnetic Calorimeter located inside the magnet coil. Muons and K_L^0's are detected using resistive plate chambers embedded in the iron magnetic flux return. Charged particles are identified using specific ionisation losses in the tracking chamber and identification information from the Aerogel Cherenkov Counters and Time of Flight Counters. The Belle detector is described in detail elsewhere [16].

At the $\Upsilon(4S)$, $B\bar{B}$ pairs are produced with no accompanying particles. As a result, the B meson has an energy that is equal to $E_{\rm beam} = \sqrt{s}/2$. B mesons are identified using the beam constrained mass $M_{bc} = \sqrt{E^2_{\rm beam} - p^2_B}$ and the energy difference $\Delta E = E_{\rm beam} - E_B$, where p_B is the vector sum of the centre-of-mass (cms) momenta of the B meson decay products and E_B is their cms energy sum. The signal events for fully reconstructed B candidates peak at $\Delta E \approx 0$ and have resolution of 10 MeV. The experimental resolution in M_{bc} is typically a few times better than that for invariant mass of reconstructed B meson and is determined mostly by a precision of a measurement of $E_{\rm beam}$.

3. Theory predictions for *P*-wave excitations of $c\bar{u}$ and $c\bar{s}$ mesons and recent experimental status

The potential models of a heavy–light Qq system employ the Heavy Quark Symmetry [5, 6]. As the heavy quark's mass increases its motion in a meson decreases and the properties of meson become governed by the dynamics of the light quark. Mesons with one heavy quark become similar to the hydrogen atom. Heavy quark acts as a static source of chromoelectric field, chromomagnetic interaction (gluon-exchange) vanishes. The light degrees of freedom are insensitive to m_Q, thus the heavy quark spin $\vec{s}_Q$ decouples from the light quark. The spin quantum numbers of light degrees of freedom (total angular momentum of the light quark $\vec{j}_q = \vec{L} + \vec{s}_q$) and that of the heavy quark ($\vec{s}_Q$) are separately conserved and thus become good quantum numbers. The total angular momentum of the meson is: $\vec{J} = \vec{j}_q + \vec{s}_Q = \vec{j}_q \pm 1/2$. States with the equal $\vec{j}_q$ but different $\vec{J}$ are degenerated. Since the heavy quark symmetry is only approximate symmetry relativistic corrections must be taken into account. After this the hyperfine splitting emerges for degenerated states ($1/m_Q$ effect).

There are four P-wave states with the following spin-parity (J^P) and light quark angular momenta: $0^+(\vec{j}_q = 1/2)$, $1^+(\vec{j}_q = 1/2)$, $1^+(\vec{j}_q = 3/2)$, $2^+(\vec{j}_q = 1/2)$. For $c\bar{u}$ system they are labelled as $D^\star_0$, D'_1, D_1 and $D^\star_2$, respectively. The energy levels of $c\bar{u}$ system excitations are shown in Fig. 1. The two $\vec{j}_u = 3/2$ states are narrow with widths of order 20 MeV and have been observed by ARGUS [17] and CLEO [18]. Their measured masses agree with the potential model predictions. The products of branching fractions of these narrow $D^{\star\star}$ states observed in $B \to D^\star\pi\pi$ decay have been measured by CLEO to be:

$$\begin{aligned}
\mathcal{B}(B^- \to D^0_1\pi^-) \times \mathcal{B}(D^0_1 \to D^{\star+}\pi^-) &= (7.8 \pm 1.9) \times 10^{-4}\,, \\
\mathcal{B}(B^- \to D^{\star 0}_2\pi^-) \times \mathcal{B}(D^{\star 0}_2 \to D^{\star+}\pi^-) &= (4.2 \pm 1.7) \times 10^{-4}\,.
\end{aligned}$$

QCD sum rules predict [19] the dominance of a tensor $D^{\star\star}(\vec{j}_q = 3/2)$ state in $B \to D^{\star\star} l\nu$ semileptonic decays. However the total branching fraction $\mathcal{B}(B \to D^{\star}\pi l\nu) = 2.6 \pm 0.5\%$ as measured by ALEPH and DELPHI, seems to be not saturated by the contribution of the narrow resonances, $(0.86 \pm 0.37)\%$ [20] Therefore a large contribution of broad or non-resonant $D^{(\star)}\pi$ structures is not excluded. Such broad structures could be the remaining $\vec{j}_u = 1/2$ states. They are expected to have large widths ($O(100)$ MeV) because of S-wave $D^{(\star)}\pi$ decays. They have not been observed directly till last year.

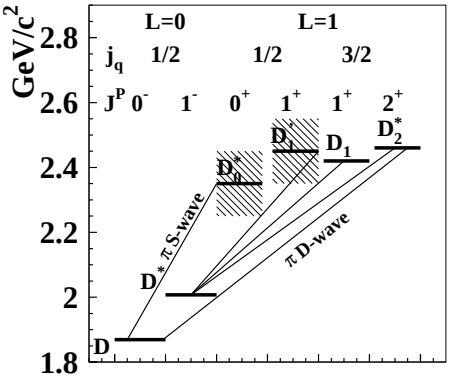

Fig. 1. The potential model prediction for $c\bar{u}$ levels.

For $c\bar{s}$ system the P-wave excitations status is similar as in the $D^{\star\star}$ case. An experimental evidence exist [21, 22] for the narrow $D_{s1}(2536)$ and $D_{sJ}(2573)$ states which decay dominantly to $D^{\star}K$ and DK, respectively. They are identified with the 1^+ and 2^+ members of the $\vec{j}_s = 3/2$ doublet. For the remaining two states, those with $\vec{j}_s = 1/2$ labelled as D_{s0}, D'_{s1}, theoretical models typically predict masses between 2.4–2.6 GeV [5,6]. Both states could decay by a kaon emission, therefore their widths could be large making their observation difficult.

4. New D^{**} resonances

The studies of $B^- \to D^+\pi^-\pi^-$ and $B^- \to D^{\star+}\pi^-\pi^-$ decays in Belle were based on 65.4 million $B\bar{B}$ pairs. These reactions at the quark level are dominated by the tree-level $b \to cW^- \to c\bar{u}d$ transition with an external or internal (colour suppressed) W emission. Because of the quark content of final states the $c\bar{u}$ mesons are expected to be easily created in such processes.

The D and $D^{\star}$ mesons are reconstructed in the decay modes: $D^0 \to K^-\pi^+, K^-\pi^+\pi^+\pi^-$, $D^+ \to K^-\pi^+\pi^+$, $D^{\star+} \to D^0\pi^+$. The detailed description of the analysis can be found in [11]. B candidates events are identified by

their beam constrained mass M_{bc} and cms energy difference ΔE (described in Section 1). The M_{bc} and ΔE distributions for $B^- \to D^+\pi^-\pi^-$ and $B^- \to D^{\star+}\pi^-\pi^-$ are shown in Fig. 2 and Fig. 3, respectively.

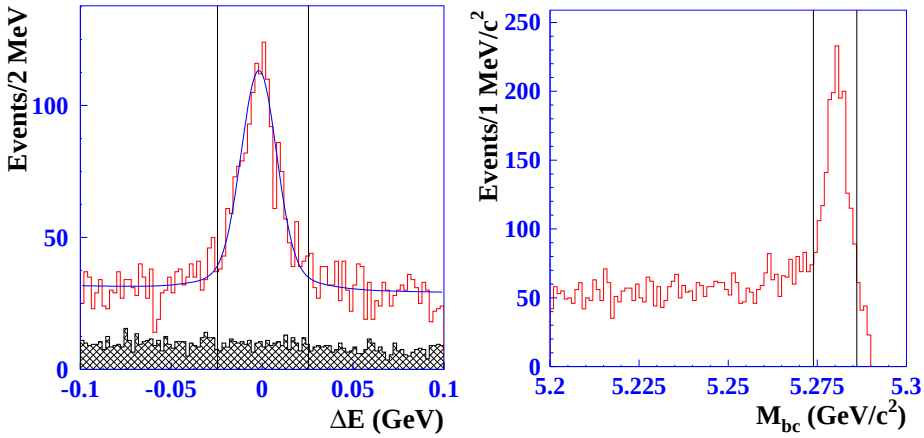

Fig. 2. The M_{bc} and ΔE distributions for $B^- \to D^+\pi^-\pi^-$ candidates. M_{bc} is plotted for events satisfying selection cut: $|\Delta E| < 25$ MeV, ΔE distribution contains only B candidates with $|M_{bc} - M_B| < 6$ MeV. Vertical lines show the signal region, superimposed curve is fit result. The hatched histogram represents background from the D mass sideband.

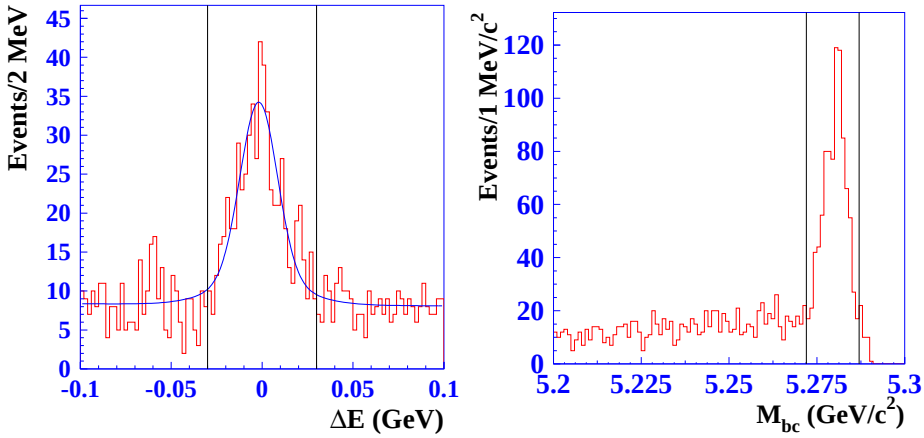

Fig. 3. The M_{bc} and ΔE distributions for $B^- \to D^{\star+}\pi^-\pi^-$ candidates. M_{bc} is plotted for events satisfying: $|\Delta E| < 30$ MeV, ΔE distribution for B candidates with $|M_{bc} - M_B| < 6$ MeV. Vertical lines show the signal region, superimposed curve is fit result.

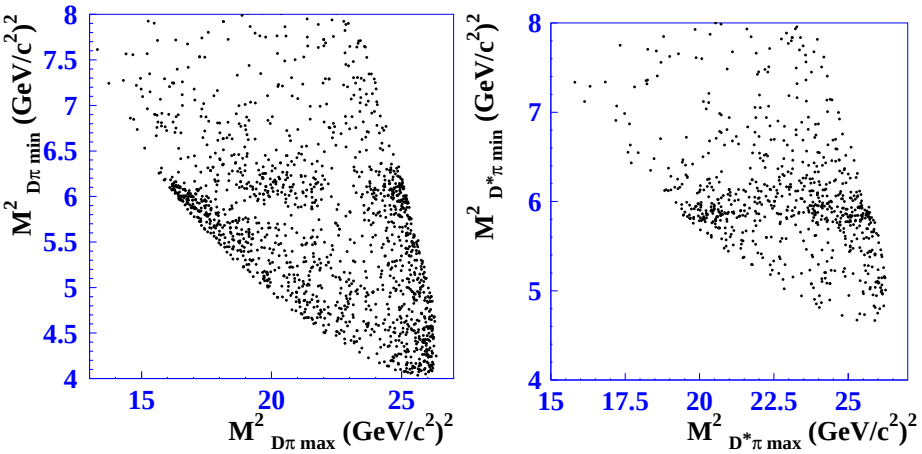

Fig. 4. The Dalitz plot for $B^- \to D^+\pi^-\pi^-$ (a) and $B^- \to D^{\star+}\pi^-\pi^-$ (b), for events from the signal region.

About 1100 $B^- \to D^+\pi^-\pi^-$ and 550 $B^- \to D^{\star+}\pi^-\pi^-$ decays have been reconstructed and their branching fractions have been measured to be:

$$\begin{aligned} \mathcal{B}(B^- \to D^+\pi^-\pi^-) &= (1.02 \pm 0.04 \pm 0.15) \times 10^{-3}\,, \\ \mathcal{B}(B^- \to D^{\star+}\pi^-\pi^-) &= (1.25 \pm 0.08 \pm 0.22) \times 10^{-3}\,. \end{aligned}$$

Relatively large signal samples observed at moderate backgrounds enabled the Dalitz plot analysis for those three-body decays. Two invariant masses are used as independent variables in the Dalitz plot. Since the final state contains two identical pions, the pair $M^2_{\rm min}$ and $M^2_{\rm max}$, a maximal and minimal $D^{(\star)}\pi$ mass, is used.

The $M^2_{D^{(\star)}\pi\ \rm min}$ *versus* $M^2_{D^{(\star)}\pi\ \rm max}$ Dalitz for $B^- \to D^{(\star)+}\pi^-\pi^-$ signal region events are shown in Fig. 4. The minimal $D^{(\star)}\pi$ mass distributions for the signal and sideband ($30 < |\Delta E| < 100$ MeV) events are shown in Figs. 5(a), 6(a). Narrow peaks at $\approx$2.4 GeV and broad enhancements over the backgrounds are observed.

An unbinned maximum likelihood fit to the Dalitz plot is performed to extract the amplitudes and phases of different intermediate states. The event density function is the sum of the signal and background functions. The background shape is obtained from the fit of a two-dimensional function to the sideband distribution. The number of background events in the signal region is scaled according to relative areas of the signal and the sideband regions.

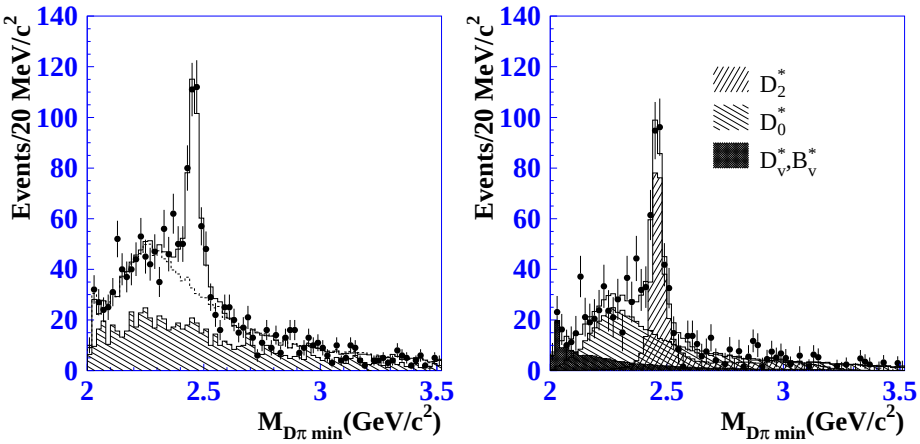

Fig. 5. (a) The minimal $D\pi$ mass distribution of $B^- \to D^+\pi^-\pi^-$ candidates. The points correspond to the signal-region events, the hatched histogram shows the background obtained from the sidebands. The open histogram is the result of the fit. (b) The background-subtracted $D\pi$ mass distribution. The points correspond to the signal-region events, hatched histograms show different contributions, the open histogram represents the coherent sum of all contributions.

The signal-event density function $S(M^2_{D^{(\star)}\pi\,\mathrm{min}}, M^2_{D^{(\star)}\pi\,\mathrm{max}})$ contains contributions of possible intermediate states, included as a coherent sum of corresponding amplitudes together with a constant amplitude describing possible non-resonant $D^{(\star)}\pi$ component.

In the $D^+\pi^-\pi^-$ final state a combination of the $D\pi$ can form either a tensor meson $D_2^{\star 0}$ or a scalar state $D_0^{\star 0}$. The axial vector mesons D_1^0 and $D_1^{\prime 0}$ cannot decay to two pseudoscalars because of the angular momentum and parity conservation. Also the virtual hadrons can be produced in this combinations, such as virtual $D_v^{\star 0}$ (the real $D^{\star 0}$ cannot decay to $D^+\pi^-$ because of its mass that is lower than that of $D^+\pi^-$) and $B_v^\star$ ($B \to B_v^\star\pi$ and $B_v^\star \to D\pi$). Resonances are described by a relativistic Breit–Wigner (A) with a mass dependent width and an angular dependence that corresponds to the spin of the intermediate and final state particles. The signal-events density function is:

$$S(M^2_{D\pi\,\mathrm{min}}, M^2_{D\pi\,\mathrm{max}}) = \left| \sum_i a_i e^{i\phi_i} A^{(i)}(M^2_{D\pi\,\mathrm{min}}, M^2_{D\pi\,\mathrm{max}}) + a_3 e^{i\phi_3} \right|^2 \otimes \mathcal{R}\,,$$

where a_i and ϕ_i denote amplitudes for the intermediate states and their relative phases. $\otimes\mathcal{R}$ represents a convolution of the signal function with the experimental resolution that is obtained from MC simulation.

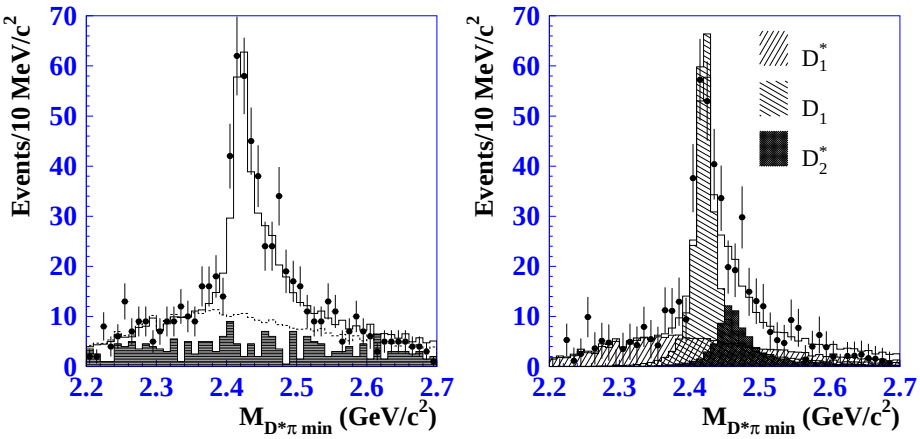

Fig. 6. (a) The minimal $D^\star\pi$ mass distribution of $B^- \to D^{\star+}\pi^-\pi^-$ candidates. The points correspond to experimental data from the signal region, the hatched histogram shows the background obtained from the sidebands, the open histogram is MC simulation with the amplitudes and parameters obtained from the fit, the dashed histogram shows contribution of the broad resonance. (b) The background-subtracted $D^\star\pi$ mass distribution. The points correspond to the signal-region events, hatched histograms show different contributions, the open histogram represents the coherent sum of all contributions.

The $D^{\star\star}$ resonances parameters, as well as the amplitudes for the intermediate states and relative phases, are free parameters of the fit. Adding the virtual $D_v^{\star 0}$ and $B_v^\star$ amplitudes improves the likelihood significantly. A constant non-resonant term (a_3) does not substantially change the likelihood, thus it is neglected. The maximum likelihood values are significantly worse if the broad scalar resonance is excluded from the fit or its spin $\neq 0$ is assumed. The scalar state mass and width are found to be:

$$M_{D_0^{\star 0}} = (2308 \pm 17 \pm 15 \pm 28)\ \mathrm{MeV}/c^2\,,$$
$$\Gamma_{D_0^{\star 0}} = (276 \pm 21 \pm 18 \pm 60)\ \mathrm{MeV}\,.$$

The mass and width of the narrow tensor state are determined to be:

$$M_{D_2^{\star 0}} = (2461.6 \pm 2.1 \pm 0.5 \pm 3.3)\ \mathrm{MeV}/c^2\,,$$
$$\Gamma_{D_2^{\star 0}} = (45.6 \pm 4.4 \pm 6.5 \pm 1.6)\ \mathrm{MeV}\,.$$

The error values correspond to statistical, systematic and model-dependent errors respectively. The value of the $D_2^{\star 0}$ width is larger than the world average of 23 ± 5 MeV [23]. The measurements included in the world average

assumed no interference effects. The width is consistent with the recent result of FOCUS [24]: 30.5 ± 4.2 MeV. The background subtracted $D\pi$ mass distribution is shown in Fig. 5(b), together with the fit predictions.

The $D^\star\pi$ final state can include contribution from the narrow $D_2^{\star 0}$ and D_1^0 states and the broad $D_1^{\prime 0}$ state. Since $D^\star$ is a vector particle the two additional (besides $M^2_{D^\star\pi\ \mathrm{min}}$ and $M^2_{D^\star\pi\ \mathrm{max}}$) variables are needed to describe final states. The variables are chosen to be the angle α between pions from the $D^{\star\star}$ and $D^\star$ in the $D^\star$ rest frame, and the azimuthal angle γ of the pion from the $D^\star$ decay relative to the $B \to D^\star\pi\pi$ decay plane. The signal function is a function of four parameters: $S(M^2_{D^\star\pi\ \mathrm{min}}, M^2_{D^\star\pi\ \mathrm{max}}, \alpha, \gamma)$ and includes amplitudes of intermediate tensor $D_2^\star$ and two axial vector mesons $D_1^{'}$ and D_1. Observed 1^+ states can be a mixture of two pure states. The possibility of the mixing is accounted for in the fit by introducing the mixing angle between the two 1^+ states and the relative phase between pure states amplitudes.

The amplitudes and phases of the intermediate states are obtained from the unbinned maximum likelihood fit in the four-dimensional space. Also in this case adding of a virtual D_v and $B_v^\star$ improves the likelihood, the non-resonant term does not influence the result. Inclusion of a broad resonance with the 1^+ quantum numbers improves the likelihood significantly. A fit with contribution of broad resonance with other quantum number such as 0^-, 1^- or 2^- makes likelihood significantly worse. The $D_2^\star$ mass and width have been fixed to the values obtained from $D\pi\pi$ analysis. The new broad 1^+ $D_1^{\prime 0}$ state is observed with a statistical significance exceeding 10σ. Its mass and width are determined to be:

$$\begin{aligned} M_{D_1^{\prime 0}} &= (2427 \pm 26 \pm 20 \pm 15)\ \mathrm{MeV}/c^2\,, \\ \Gamma_{D_1^{\prime 0}} &= (384^{+107}_{-75} \pm 24 \pm 70)\ \mathrm{MeV}\,. \end{aligned}$$

Observation of a similar state was reported by CLEO [25] with parameters: $M_{D_1^{\prime 0}} = (2461^{+48}_{-42})$ MeV/c^2, $\Gamma_{D_1^{\prime 0}} = (290^{+110}_{-90})$ MeV. For the D_1 meson the following parameters have been obtained:

$$\begin{aligned} M_{D_1^0} &= (2421.4 \pm 1.5 \pm 0.4 \pm 0.8)\ \mathrm{MeV}/c^2\,, \\ \Gamma_{D_1^0} &= (23.7 \pm 2.7 \pm 0.2 \pm 4.0)\ \mathrm{MeV}\,. \end{aligned}$$

The background-subtracted $D^\star\pi$ mass distribution, together with a coherent sum of all amplitudes and contributions from separate states superimposed, is shown in Fig. 6(b).

The products of the branching fractions for the $D^{\star\star}$ states are measured:

$$\begin{aligned}
\mathcal{B}(B^- \to D_2^{\star 0}\pi^-) \times \mathcal{B}(D_2^{\star 0} \to D^+\pi^-) &= (3.4 \pm 0.3 \pm 0.6 \pm 0.4) \times 10^{-4}\,, \\
\mathcal{B}(B^- \to D_0^{\star 0}\pi^-) \times \mathcal{B}(D_0^{\star 0} \to D^+\pi^-) &= (6.1 \pm 10.6 \pm 0.9 \pm 1.6) \times 10^{-4}\,, \\
\mathcal{B}(B^- \to D_2^{\star 0}\pi^-) \times \mathcal{B}(D_2^{\star 0} \to D^{\star +}\pi^-) &= (1.8 \pm 0.3 \pm 0.3 \pm 0.2) \times 10^{-4}\,, \\
\mathcal{B}(B^- \to D_1^{0}\pi^-) \times \mathcal{B}(D_1^{0} \to D^{\star +}\pi^-) &= (6.8 \pm 0.7 \pm 1.3 \pm 0.3) \times 10^{-4}\,, \\
\mathcal{B}(B^- \to D_1^{\prime 0}\pi^-) \times \mathcal{B}(D_1^{\prime 0} \to D^{\star +}\pi^-) &= (5.0 \pm 0.4 \pm 1.0 \pm 0.4) \times 10^{-4}\,.
\end{aligned}$$

These measurements show that the narrow resonances comprise $(36 \pm 6)\%$ of $D\pi\pi$ decays and $(63 \pm 6)\%$ of $D^\star\pi\pi$ decays. This result is inconsistent with the QCD sum rule that predicts the dominance of the narrow states in $B \to D^\star\pi\pi$ decays [19].

5. Observation of new D_{sJ} states

The measurements of quantum numbers and production properties of the new D_{sJ} mesons is crucial for understanding of their nature. Belle has observed the $D_{sJ}^+(2317)$ and $D_{sJ}^+(2457)$ states in continuum $c\bar{c}$ production process and in decays of B mesons. Their masses, widths and branching fractions in dipion and radiative decay modes have been determined.

5.1. Production in continuum processes $e^+e^- \to D_{sJ}X$

The D_{sJ} resonances are studied in $D_s^+\pi^0$ and $D_s^{\star +}\pi^0$ final states as well as in dipion $D_s^+\pi^+\pi^-$ and radiative $D_s^+\gamma$ decay modes. The D_s^+ is reconstructed in $D_s^+ \to \phi\pi^+$ and $\phi \to K^+K^-$ decay chain, $D_s^{\star +}$ mesons in the $D_s^+\gamma$ final state. To remove combinatorial background from $B\bar{B}$ events only the high-momenta $D_s^{(\star)+}\pi^0$ combinations are considered ($p^\star(D_s^{(\star)+}\pi^0) > 3.5$ GeV in the $\Upsilon(4S)$ rest frame).

The $\Delta M(D_s^{(\star)+}\pi^0) = M(D_s^{(\star)+}\pi^0) - M(D_s^{(\star)+})$ mass difference distributions shown in Fig. 7. The peaks corresponding to $D_{sJ}^+(2317) \to D_s^+\pi^0$ (a) and $D_{sJ}^+(2457) \to D_s^{\star +}\pi^0$ are seen. The cross-feed between both states is possible because the signal peaks in both decays modes appear at nearly the same ΔM, thus an average π^0 momentum is similar in both decays. The $D_{sJ}^+(2317)$ produces a reflection of a few MeV above $D_{sJ}^+(2457)$ (Fig. 7(b)) if D_s^+ and π^0 from $D_{sJ}^+(2317)$ are combined with a random photon. The $D_{sJ}^+(2457)$ produces a reflection peak just below the mass of $D_{sJ}^+(2317)$, when a photon from the $D_s^{\star +}$ decay is not reconstructed (the smaller peak in Fig. 8(a)). The cross-feed background in the $D_{sJ}^+(2317)$ region is separated using the background shape modelled from the Monte Carlo. In the $D_{sJ}^+(2457)$ case the feed-down background is removed by subtracting from the $D_s^{\star +}$ signal distribution the background estimated from the $D_s^{\star +}$ sideband.

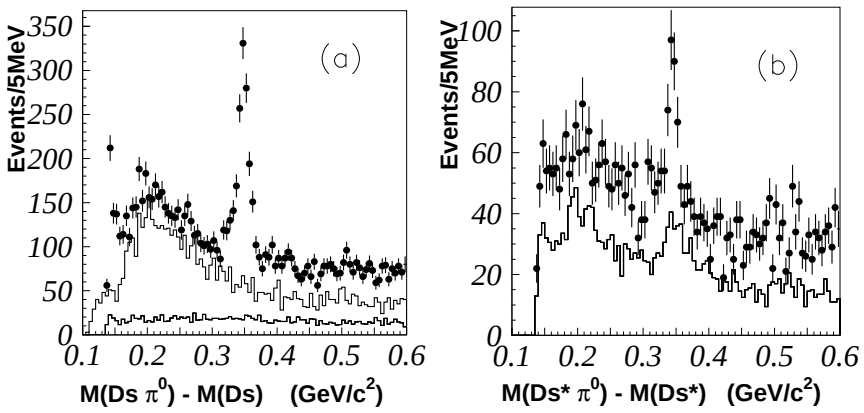

Fig. 7. (a) The $\Delta M(D_s^+\pi^0)$ mass difference distribution. The histograms show data from D_s^+ (solid) and π^0 (dotted) sideband regions. (b) The $\Delta M(D_s^{\star+}\pi^0)$ mass difference distribution. Data from $D_s^{\star+}$ sideband are represented by histogram.

Figure 8 shows the $\Delta M(D_s^{(\star)+}\pi^0)$ distributions together with the results of the fit. The signal yields of $761 \pm 44(\text{stat}) \pm 30(\text{syst})$ and $126 \pm 25(\text{stat}) \pm 12(\text{syst})$ have been obtained for the $D_{sJ}^+(2317)$ and $D_{sJ}^+(2457)$, respectively. The widths obtained in the fit are consistent with MC expectations for a zero intrinsic width. Upper limits for the natural widths have been set to be $\Gamma(D_{sJ}^+(2317)) \leq 4.6$ MeV/c^2 and $\Gamma(D_{sJ}^+(2317)) \leq 5.5$ MeV/c^2 (90%C.L.). The results for the masses are the following:

$$\begin{aligned} M(D_{sJ}(2317)) &= 2317.2 \pm 0.5(\text{stat}) \pm 0.9(\text{syst}) \text{ MeV}/c^2\,, \\ M(D_{sJ}(2457)) &= 2456.5 \pm 1.3(\text{stat}) \pm 1.3(\text{syst}) \text{ MeV}/c^2\,. \end{aligned}$$

The $M(D_{sJ}^+(2317))$ result is consistent with the BaBar [1] and CLEO [2] results. The $M(D_{sJ}^+(2457))$ measurement agrees with the BaBar result [26] and is significantly lower than that found in CLEO.

No significant signal in the $D_{sJ}^+(2457)$ region of the $\Delta M(D_s^+\pi^0)$ distribution indicates an absence of the $D_{sJ}(2457)$ decay to a pseudoscalar pair. Such decay is allowed for states with a parity $P = (-1)^J$, thus 0^+ and 1^- assignments are ruled out for the $D_{sJ}(2457)$.

The $\Delta M(D_s^+\gamma) = M_{D_s^+\gamma} - M_{D_s^+}$ distribution is shown in Fig. 9(a). No signal is found in the $D_{sJ}(2317)$ region. The peak at $\Delta M(D_s^+\gamma) \approx 490$ MeV/c^2 corresponds to the $D_{sJ}(2457)$ signal. The fit predicts $152 \pm 18(\text{stat})$ $D_{sJ}(2457) \to D_s^+\gamma$ events. From this the branching fraction ratio is determined:

$$\frac{\text{BR}\,(D_{sJ}^+(2457) \to D_s^+\gamma)}{\text{BR}\,(D_{sJ}^+(2457) \to D_s^{\star+}\pi^0)} = 0.55 \pm 0.13(\text{stat}) \pm 0.08(\text{syst})\,.$$

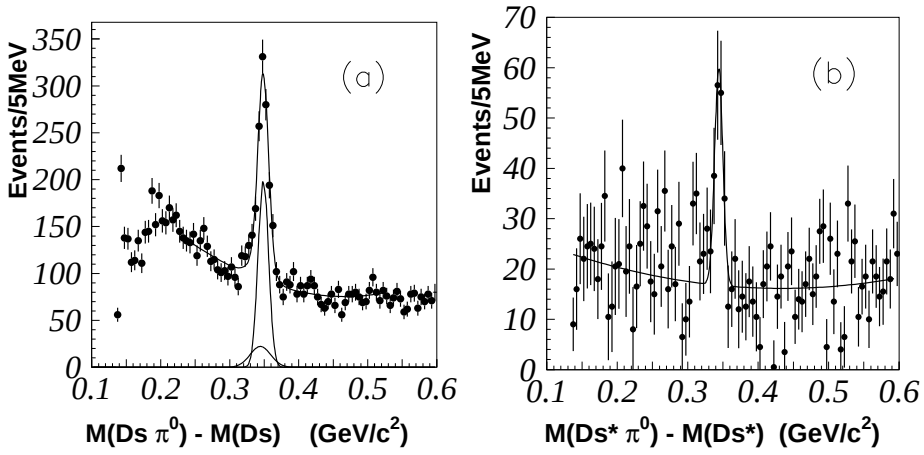

Fig. 8. (a) The $\Delta M(D_s^+\pi^0)$ mass difference distribution. The narrow Gaussian peak is the $D_{sJ}^+(2317)$ fitted signal, the smaller one corresponds to feed-down background from the $D_{sJ}^+(2457)$. (b) The $\Delta M(D_s^{\star+}\pi^0)$ mass difference distribution (after subtraction of the $D_s^{\star+}$ sideband from the signal distribution) and the fit result.

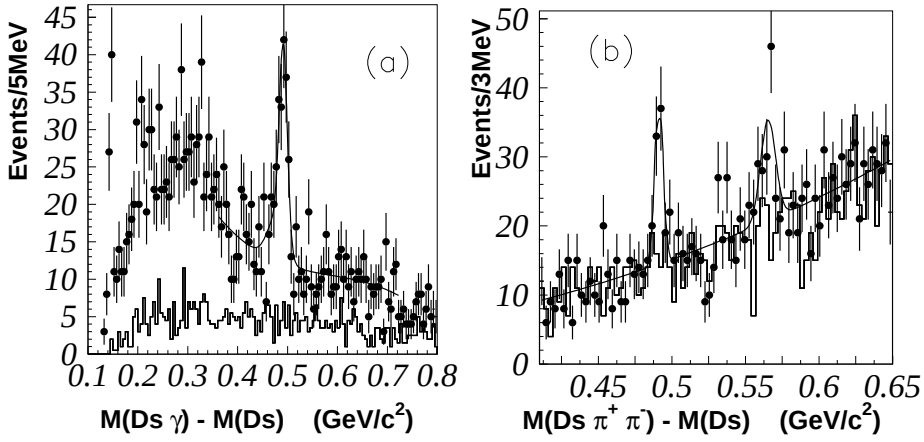

Fig. 9. The $\Delta M(D_s^+\gamma)$ (a) and $\Delta M(D_s^+\pi^+\pi^-)$ (b) mass difference distributions.

The existence of the $D_{sJ}^+(2457) \to D_s^+\gamma$ radiative decay rules out the $J^P = 0^\pm$ assignment to $D_{sJ}(2457)$. In the $D_s^{\star+}\gamma$ decay mode no significant signal is observed for the $D_{sJ}(2317)$ as well as the $DsJ(2457)$ state. Figure 9(b) shows the $\Delta M(D_s^+\pi^+\pi^-) = M_{D_s^+\pi^+\pi^-} - M_{D_s^+}$ mass difference distribution. A peak near $\Delta M(D_s^+\pi^+\pi^-) \approx 490$ MeV/c^2 corresponding to

$D_{sJ}(2457)$ and an evidence of additional peak at ≈ 570 MeV/c^2 associated with $D_{s1}(2536)$, are visible. In the $D_{sJ}(2317)$ region no peak is observed. The signal of 60 ± 12(stat) events is obtained for the $D^+_{sJ}(2457) \to D^+_s \pi^+ \pi^-$ and the branching fraction ratio has been determined:

$$\frac{\mathrm{BR}\,(D^+_{sJ}(2457) \to D^+_s \pi^+ \pi^-)}{\mathrm{BR}\,(D^+_{sJ}(2457) \to D^+_{\star s} \pi^0)} = 0.14 \pm 0.04(\mathrm{stat}) \pm 0.02(\mathrm{syst})\,.$$

The existence of the $D^+_{sJ}(2457) \to D^+_s \pi^+ \pi^-$ excludes the $D_{sJ}(2457)$ being the 0^+ state. The absence of other than $D^+_s \pi^0$ decay modes for the $D_{sJ}(2317)$ is consistent with the 0^+ spin-parity assignment.

5.2. The D_{sJ} in B meson decays

If the newly observed D_{sJ} states are ordinary $c\bar{s}$ mesons they should be easily produced in B meson decays. The decays of the type $B \to \bar{D} D_{sJ}$ are expected to be the dominant exclusive D_{sJ} production mechanisms in B decay. These decays proceed via a $b \to cW$ transition, where the W materialises in the D_{sJ}. Since the spin of the parent B meson is fixed, the angular analysis of this decay can be performed to unambiguously determine the spin-parity of the D_{sJ} states. HQET predicts that P-wave mesons with the light-quark angular momentum $j_q = 1/2$ should be more frequently produced in B decays than mesons with $j_q = 3/2$ [27]. Thus, the observation of $B \to \bar{D} D_{sJ}$ would provide additional support for the P-wave nature of these states.

Search for the $B \to \bar{D} D_{sJ}(2317)$ and $B \to \bar{D} D_{sJ}(2457)$ is based on a sample of $124 \times 10^6 B\bar{B}$ pairs collected with the Belle detector. The $\bar{D}$ denotes $\bar{D}^0$ (reconstructed in $K^+\pi^-$, $K^+\pi^-\pi^+\pi^-$, $K^+\pi^-\pi^0$ decay channels) or D^- (in $K^+\pi^-\pi^-$ mode). The D_{sJ} candidates are reconstructed from $D_s^{(\star)}$ mesons and a π^0, γ or $\pi^+\pi^-$ pair. The mass difference $M(D_{sJ}) - M(D_s^{(\star)})$ is used to select candidates. The B mesons are formed by combining $\bar{D}$ and D_{sJ} and are identified by their c.m. energy difference ΔE and the beam constrained mass M_{bc}. Only the events with $|\Delta E| < 0.02$ GeV and $5.272 < M_{bc} < 5.288\mathrm{GeV}/c^2$ are selected. The ΔE and $M(D_{sJ})$ invariant mass distributions of D_{sJ} candidates for $B \to \bar{D} D_{sJ}$ are shown in Fig. 10.

Clear signals are observed for the $B \to \bar{D} D_{sJ}(2317)$ $[D_{sJ}(2317) \to D_s \pi^0]$ and $B \to \bar{D} D_{sJ}(2457)$ $[D_{sJ}(2457) \to D^\star_s \pi^0,\ D_s \gamma]$ final states. The measured masses for the $D_{sJ}(2317)$ and $D_{sJ}(2457)$ are $(2319.8 \pm 2.1 \pm 2.0)$ MeV/c^2 and $(2459.2 \pm 1.6 \pm 2.0)$ MeV/c^2, respectively. The fitted widths are consistent with zero intrinsic width. For other D_{sJ} decay channels significant signals are not seen.

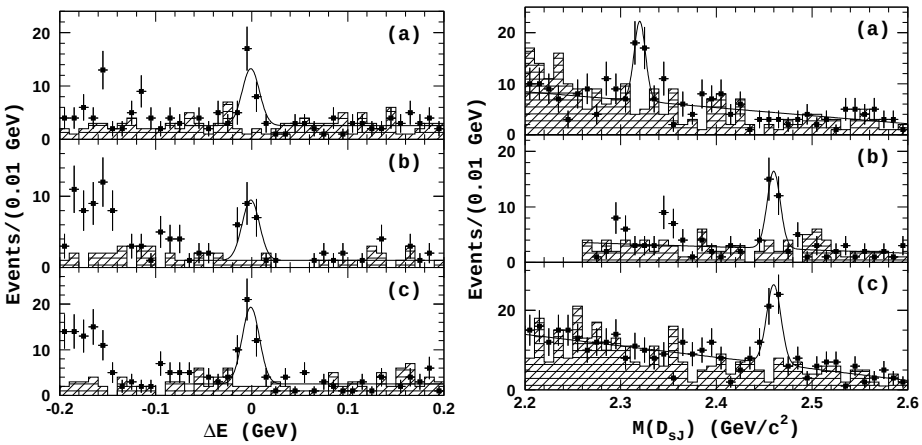

Fig. 10. The ΔE (left) and $M(D_{sJ})$ (right) distributions for the $B \to \bar{D} D_{sJ}$ candidates: (a) $D_{sJ}(2317) \to D_s \pi^0$ (b) $D_{sJ}(2457) \to D_s^\star \pi^0$ (c) $D_{sJ}(2457) \to D_s^\star \gamma$. Points with errors show the experimental data, hatched histograms represent distributions for events in the $M(D_{sJ})$ and ΔE sidebands, respectively. Curves are the results of the fits.

The branching fractions (or 90 % C.L. upper limits) measured for $B \to \bar{D} D_{sJ}(2317)$ and $B \to \bar{D} D_{sJ}(2317)$ are presented in the Table.

TABLE

The measured branching fractions with corresponding statistical significances.

Decay channel	$\mathcal{B}$, 10^{-4}	Significance
$B \to \bar{D} D_{sJ}(2317)$ $[D_{sJ}(2317) \to D_s \pi^0]$	$8.5^{+2.1}_{-1.9} \pm 2.6$	6.1σ
$B \to \bar{D} D_{sJ}(2317)$ $[D_{sJ}(2317) \to D_s^\star \gamma]$	$2.5^{+2.0}_{-1.8}$ (< 7.5)	1.8σ
$B \to \bar{D} D_{sJ}(2457)$ $[D_{sJ}(2457) \to D_s^\star \pi^0]$	$17.8^{+4.5}_{-3.9} \pm 5.3$	6.4σ
$B \to \bar{D} D_{sJ}(2457)$ $[D_{sJ}(2457) \to D_s \gamma]$	$6.7^{+1.3}_{-1.2} \pm 2.0$	7.4σ
$B \to \bar{D} D_{sJ}(2457)$ $[D_{sJ}(2457) \to D_s^\star \gamma]$	$2.7^{+1.8}_{-1.5}$ (< 7.3)	2.1σ
$B \to \bar{D} D_{sJ}(2457)$ $[D_{sJ}(2457) \to D_s \pi^+ \pi^-]$	< 1.6	—
$B \to \bar{D} D_{sJ}(2457)$ $[D_{sJ}(2457) \to D_s \pi^0]$	< 1.8	—

The helicity distribution for the $D_{sJ}(2457) \to D_s \gamma$ decay has been studied. The helicity angle $\theta_{D_s\gamma}$ is defined as the angle between the $D_{sJ}(2457)$ momentum in the B meson rest frame and the D_s momentum in the $D_{sJ}(2457)$ rest frame. The $\theta_{D_s\gamma}$ distribution (shown in Fig. 11) is consistent with expectations for the $J = 1$ hypothesis for the $D_{sJ}(2457)$ (χ^2/n.d.f. = 5/6),

and it is not for the $J = 2$ hypothesis(χ^2/n.d.f. = 44/6). The $J = 0$ is already ruled out by the conservation of angular momentum and parity in $D_{sJ}(2457) \to D_s\gamma$.

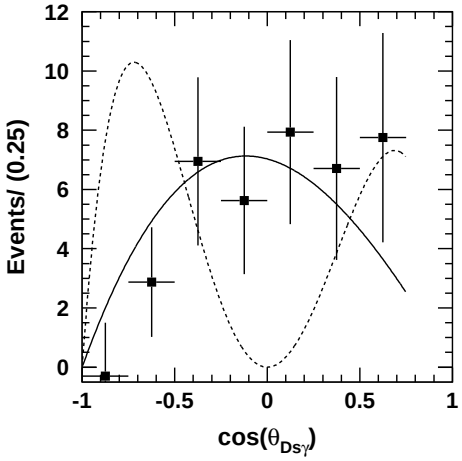

Fig. 11. The $D_{sJ}(2457) \to D_s\gamma$ helicity distribution. The points with error bars are the results of fits to δE spectra for experimental events. Solid and dashed curves are MC predictions for the $J = 1$ and $J = 2$ hypotheses, respectively.

6. Discovery of the $X(3872)$ and its properties studies

The narrow charmonium like state decaying to $\pi^+\pi^- J/\psi$ has been observed by Belle in $B^\pm \to K^\pm\pi^+\pi^- J/\psi$ using a 152×10^6 $B\bar{B}$ events sample. The J/ψ is reconstructed from well identified e^+e^- or $\mu^+\mu^-$ pairs with an invariant mass $3.077 < M_{l^+l^-} < 3.117$ GeV. Candidate $B^\pm \to K^\pm\pi^+\pi^- J/\psi$ mesons are identified using their c.m. energy difference ΔE and the beam constrained mass M_{bc}. The signal region is defined as $|\Delta E| < 0.03$ GeV and $5.271 < M_{bc} < 5.289$ GeV/c^2. Fig. 12(a) shows the distribution of $\Delta M = M(\pi^+\pi^- l^+l^-) - M(l^+l^-)$ for events in the ΔE–M_{bc} signal region. In addition to a large peak at 0.589 GeV corresponding to $\psi' \to \pi^+\pi^- J/\psi$, a significant spike at 0.775 GeV is visible. Its ΔM corresponds to a mass $M(\pi^+\pi^- J/\psi) \approx 3.872$ MeV. Fig. 12(b) shows the same distribution for sample of generic MC events where all known particles are simulated. The prominent ψ' peak is observed and the smaller peak is not seen, therefore it cannot be due to a reflection from known states.

A simultaneous unbinned maximum likelihood fit to the ΔE, M_{bc} and $M_{\pi^+\pi^- J/\psi}$ distributions is made for the data in the $M = 3872$ MeV region. The M_{bc}, $M_{\pi^+\pi^- J/\psi}$ and ΔE distributions for the $X(3872) \to \pi^+\pi^- J/\psi$ signal region are shown in Fig. 13, together with the fit result. The signal

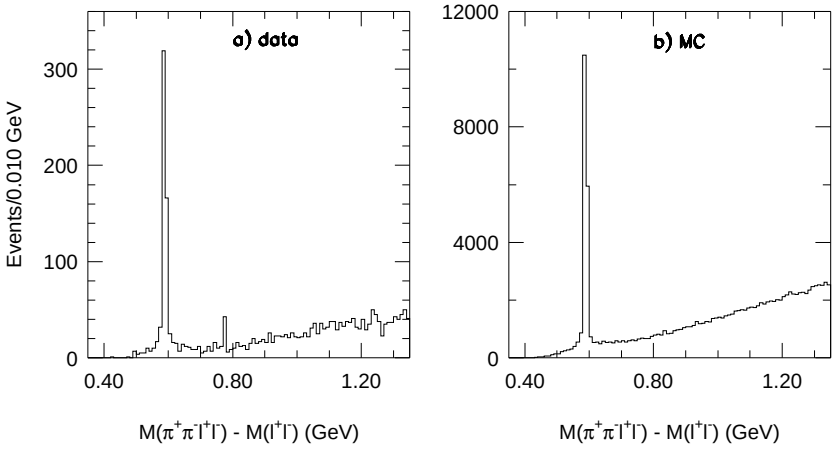

Fig. 12. The distribution of $\Delta M = M(\pi^+\pi^- l^+ l^-) - M(l^+ l^-)$ for selected events in the ΔE–M_{bc} signal region for (a) Belle data (b) generic $B\bar{B}$ MC events.

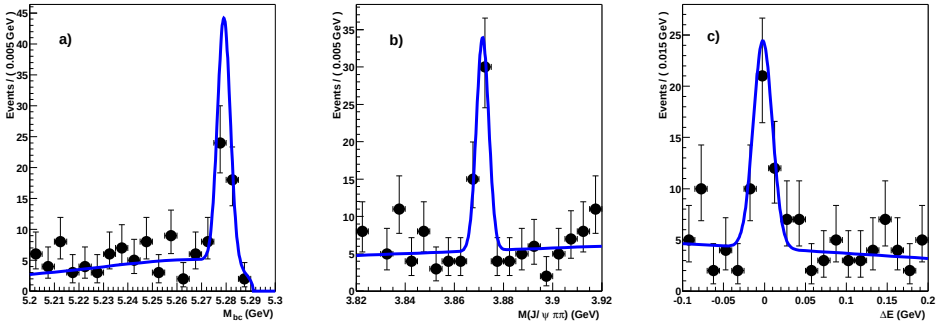

Fig. 13. Signal-band projections of (a) M_{bc}, (b) $M_{\pi^+\pi^- J/\psi}$ and (c) ΔE for the $X(3872) \to \pi^+\pi^- J/\psi$ signal region with the results of the unbinned fit superimposed.

yield of 35.7 ± 6.8 with a statistical significance of 10.3σ has been obtained for the $X(3872)$ state. A similar fit has been performed to the data in the ψ' region to obtain the mass scale calibration. The $X(3872)$ mass is determined relative to the ψ' mass and is found to be:

$$M_X = 3872.0 \pm 0.6(\text{stat}) \pm 0.5(\text{syst}) \text{ MeV}\,.$$

The measured width of the $X(3872)$ peak is $\sigma = 2.5 \pm 0.5$ MeV, which is consistent with the MC-determined resolution and the mass resolution obtained from the fit to the ψ' signal. A 90%C.L. upper limit on the width is determined to be $\Gamma < 2.3$ MeV. The $\pi^+\pi^-$ invariant masses for the $X(3872)$ events tend to cluster near kinematic boundary, which is around the ρ^0

meson mass. Similar clustering has been observed for $\psi' \to \pi^+\pi^- J/\psi$ decays. The following ratio of products of branching fractions has been measured:

$$\frac{\mathcal{B}(B^\pm \to K^\pm X(3872)) \times \mathcal{B}(X(3872) \to \pi^+\pi^- J/\psi)}{\mathcal{B}(B^\pm \to K^\pm \psi') \times \mathcal{B}(\psi' \to \pi^+\pi^- J/\psi)} = 0.063 \pm 0.012(\text{stat}) \pm 0.007(\text{syst})\,.$$

The mass of newly observed state agrees within errors with the $D^0\bar{D}^{\star 0}$ mass threshold (3871.1 ± 1.0 MeV). This suggests that the state can be a loosely bound $D\bar{D}^\star$ multiquark "molecular state". There are also potential model predictions [5,6,15] for charmonium states with masses in the $X(3872)$ region. Thus the charmonium interpretation of the $X(3872)$ is not excluded.

Although the $X(3872)$ is above the $D\bar{D}$ mass threshold, its width is narrow and decays to $D\bar{D}$ are not seen. The following 90%C.L. upper limits have been determined [28]:

$$\begin{aligned} \mathcal{B}(B^\pm \to K^\pm X(3872)) \quad &\times \mathcal{B}(X(3872) \to D^0\bar{D}^0) < 6 \times 10^{-5}\,, \\ \mathcal{B}(B^\pm \to K^\pm X(3872)) \quad &\times \mathcal{B}(X(3872) \to D^+D^-) < 4 \times 10^{-5}\,. \end{aligned}$$

So possible charmonium assignments are only those where decays to $D\bar{D}$ are forbidden or strongly suppressed.

If the $\pi^+\pi^-$ system in $X(3872) \to \pi^+\pi^- J/\psi$ has $J^P = 0^{++}$ the most likely charmonium candidates for the $X(3872)$ are: the $h_c'(2^1P_1)$ and two triplet D-wave states, the $\psi_2(^3D_2)$ and $\psi_3(^3D_3)$. For the 1^{--} dipion case, there are three charmonium possibilities : the $\eta_c''(3^1S_0)$, the $\chi_{c1}'(2^3P_1)$ and the $\eta_{c2}(^1D_2)$, but for these assignments the $\pi^+\pi^- J/\psi$ decay would violate isospin and should be strongly suppressed. The possible charmonium state assignments for the $X(3872)$ have been analysed using ≈ 270 million $B\bar{B}$ sample [29].

For the $\psi_2(^3D_2)$ the partial width $\psi_2 \to \gamma\chi_{c1}$ (an allowed E1 transition) is expected to be more than five times larger than that for $\psi_2 \to \pi^+\pi^- J/\psi$ [30]. Similarly for the $\psi_3(^3D_3)$ a partial width for the decay of the ψ_3 charmonium state to $\gamma\chi_{c2}$ is expected to be more than twice that for the $\pi^+\pi^- J/\psi$ final state.

The $X(3872)$ signal has been searched for in the $\gamma\chi_{c1}$ and $\gamma\chi_{c2}$ decay channels, where $\chi_{c1}, \chi_{c2} \to \gamma J/\psi$. No apparent signals have been found and upper limits on the ratios of partial widths have been determined to be:

$$\begin{aligned} \frac{\Gamma(X(3872) \to \gamma\chi_{c1})}{\Gamma(X(3872) \to \pi^+\pi^- J/\psi)} \quad &< 0.89 \ (90\%\text{C.L.})\,, \\ \frac{\Gamma(X(3872) \to \gamma\chi_{c2})}{\Gamma(X(3872) \to \pi^+\pi^- J/\psi)} \quad &< 1.1 \ (90\%\text{C.L.})\,. \end{aligned}$$

These limits on the decay widths contradict expectations for the ψ_2 and ψ_3, thus these states are ruled out as the assignments for the $X(3872)$.

The h_c' ($J^{\rm PC} = 1^{+-}$) hypothesis can be tested by studying the angular distribution for the $X \to \pi^+\pi^- J/\psi$. The comparison of the measured $|\cos\theta_{J/\psi}|$ distribution ($\theta_{J/\psi}$ is the J/ψ angle in the $X(3872)$ helicity frame) with the h_c' hypothesis has $\chi^2/\text{d.o.f.} = 75/9$ and thus is ruled out with a high confidence.

The χ_{c1}' is expected to be near 3968 MeV, which is well above $D\bar{D}^\star$ threshold, and its width is expected to be hundreds of MeV. It could be the candidate for the $X(3872)$ if the potential model predictions are wrong. In this case, the $\gamma J/\psi$ transition would be dominant and its partial widths much larger than that for the isospin-violating the $\pi^+\pi^- J/\psi$ mode. Search for $X(3872) \to \gamma J/\psi$ has yielded no evidence for a signal. The 90%C.L. upper limit: $\frac{\Gamma(X(3872)\to\gamma J/\psi)}{\Gamma(X(3872)\to\pi^+\pi^- J/\psi)} < 0.40$ rules out the possibility that $X(3872)$ is the $1^{++}\chi_{c1}'$.

The η_c'' width is expected to be similar to that of the η_c, much larger than the 2.3 MeV upper limit for the $X(3872)$. For the η_{c2} the $\pi^+\pi^-\eta_c$ and γh_c decays are allowed and are expected to have widths in the range of 100's of keV, again much larger than that for the isospin-violating $\pi^+\pi^- J/\psi$ mode. Moreover, if the $X(3872)$ were the η_{c2} the observed branching fraction for $B^+ \to K^+ X(3872)$ would indicate anomalously large η_{c2} production in B decays. Thus, none of the six possible charmonium candidate states fit the measured properties of $X(3872)$.

In the context of the possibility that the $X(3872)$ might be a weakly bound $1^{++} D^0 \bar{D}^{\star 0}$ molecular state, it was suggested [31] that the decay $X(3872) \to \omega J/\psi$ should occur at about half of the strength of $X(3872) \to \pi^+\pi^- J/\psi$. Although the $X(3872)$ is below the $M_{J/\psi} + M_\omega$ mass threshold, these decays could occur via the low-mass tail of the ω. The signature of the decay would be $B \to K X(3872)$, $X(3872) \to \pi^+\pi^-\pi^0 J/\psi$, where all events have $\pi^+\pi^-\pi^0$ invariant mass near the kinematic upper limit. Search for $B \to K X(3872)$, $X(3872) \to \pi^+\pi^-\pi^0 J/\psi$ has yielded 15.4 ± 6.3 of signal events. The M_{bc} and ΔE distributions for $B \to K\pi^+\pi^-\pi^0 J/\psi$ candidates and $\pi^+\pi^-\pi^0$ invariant mass are shown in Fig. 14. The M_{bc} and ΔE distributions for events with $M(\pi^+\pi^-\pi^0) > 0.75$ GeV are shown in Fig. 15. A simultaneous to M_{bc} and ΔE distributions for those events has yielded 10.0 ± 3.6 signal events. The statistical significance of the signal, determined as a difference between the likelihood values for the best-fit and for zero-signal-yield, is 5.8σ. The ratio of $X(3872) \to \omega J/\psi$ and $X(3872) \to \pi^+\pi^- J/\psi$ partial widths has been determined to be $\frac{\Gamma(X(3872)\to\omega J/\psi)}{\Gamma(X(3872)\to\pi^+\pi^- J/\psi)} = 0.8 \pm 0.3(\text{stat}) \pm 0.1(\text{syst})$. Therefore the ratio is in good agreement with expectations of Ref. [31] and provides strong support for the $D\bar{D}^\star$ molecular state interpretation.

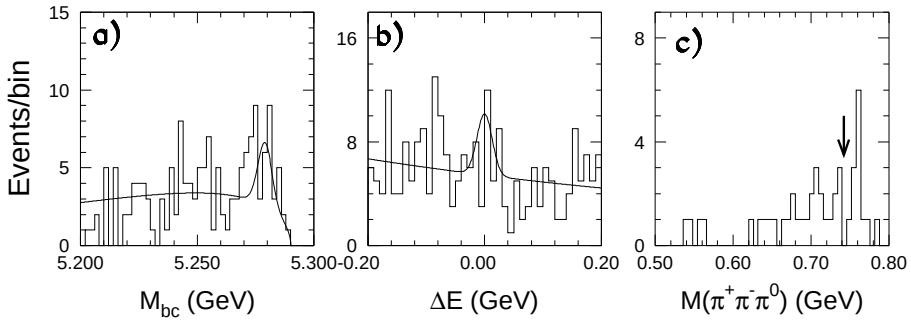

Fig. 14. (a) The M_{bc} and (b) ΔE distributions for candidate $B \to K\pi^+\pi^-\pi^0 J/\psi$ decays. The curves are result of the simultaneous fit to the two distributions. (c) $M(\pi^+\pi^-\pi^0)$ distribution for events in the M_{bc}–ΔE signal region.

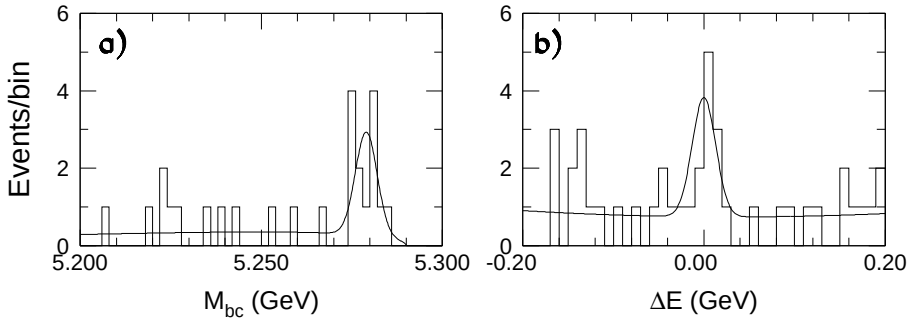

Fig. 15. (a) The M_{bc} and (b) ΔE distributions for candidate $B \to K\pi^+\pi^-\pi^0 J/\psi$ decays with $M(\pi^+\pi^-\pi^0) > 0.75$ GeV.

7. Summary

Recent discoveries of new mesons in B-factories experiments contribute to the revival of spectroscopic studies. While the properties of the two newly observed $D^{\star\star}$ states agree well with the potential models predictions, the two new D_{sJ} mesons cannot be easily accommodated within the potential model multiplets. Several non-$q\bar{q}$ assignments have been proposed for them. Their interpretation within the concept of chiral doublers is most appealing, since it is applicable to both $c\bar{u}$ ($c\bar{d}$) and $c\bar{s}$ mesons and can be tested by observing the doublers for higher excitation states.

Further studies of the properties of the $X(3872)$ are needed, but it is not excluded that this state is the first $DD^{\star}$ molecule observed.

I am thankful to my colleagues from Belle for all their work that makes this experiment so exciting. I thank the organisers of the School for inviting me and all their support. The partial support from the Polish State Committee for Scientific Research (KBN) under contract No. 2P03B 01324 is acknowledged.

REFERENCES

[1] B. Aubert *et al.* (BaBaR Collaboration), *Phys. Rev. Lett.* **90**, 242001 (2003).
[2] D. Besson *et al.* (CLEO Collaboration), *Phys. Rev.* **D68**, 032002 (2003).
[3] Y. Mikami *et al.* (Belle Collaboration), *Phys. Rev. Lett.* **92**, 012002 (2004).
[4] P. Krokovny *et al.* (Belle Collaboration), *Phys. Rev. Lett.* **91**, 262002 (2003).
[5] S. Godfrey and N. Isgur, *Phys. Rev.* **D32**, 189 (1985).
[6] E. Eichten, K. Gottfried, T. Kinoshita, K.D. Lane, T.M. Yan, *Phys. Rev.* **D21**, 203 (1980).
[7] T. Barnes, F. Close, H. Lipkin, `hep-ph/0305025`.
[8] T.E. Browder, S. Pakvasa, A. Petrov, `hep-ph/0307054`.
[9] M.A. Nowak, M. Rho, I. Zahded, *Phys. Rev.* **D48**, 4370 (1993).
[10] W. Bardeen, C. Hill, *Phys. Rev.* **D49**, 409 (1994).
[11] K. Abe *et al.* (Belle Collaboration), *Phys. Rev.* **D69**, 112002 (2004).
[12] S.-K. Choi *et al.* (Belle Collaboration), *Phys. Rev. Lett.* **91**, 262001 (2003).
[13] M. Bander, G.L. Shaw, P. Thomas, *Phys. Rev. Lett.* **36**, 695 (1976); A. De Rujula, H. Georgi, S.L. Glashov, *Phys. Rev. Lett.* **38**, 317 (1977); N.A. Törnqvist, *Z. Phys.* **C61**, 525 (1994).
[14] S. Godfrey, J. Napolitano, *Rev. Mod. Phys.* **71**, 1411 (1999).
[15] W. Buchmüller, S-H.H. Tye, *Phys. Rev.* **D24**, 132 (1981).
[16] A. Abashian *et al.* (Belle Collaboration), *Nucl. Instrum. Methods Phys. Res.*, **A479**, 117 (2002).
[17] H. Albrecht *et al.* (ARGUS Collaboration), *Phys. Lett.* **B232**, 398 (1989).
[18] J. Gronberg *et al.* (CLEO Collaboration), Conference report CLEO CONF 96-25 (1996), contributed paper to the ICHEP 96, Warsaw, Poland.
[19] A. Le Yaouanc *et al. Phys. Lett.* **B520**, 25 (2001).
[20] J. Anastassov *et al.* (CLEO Collaboration), *Phys. Rev. Lett.* **80**, 4127 (1998).
[21] J.P. Alexander *et al.* (CLEO Collaboration), *Phys. Lett.* **B303**, 377 (1993).
[22] Y. Kubota *et al.* (CLEO Collaboration), *Phys. Rev. Lett.* **72**, 1972 (1994).
[23] K. Hagiwara *et al.* (Paricle Data Group), *Phys. Rev.* **D66**, 010001 (2002).
[24] F.L. Fabbri *et al.* (FOCUS Collaboration), Presented at ICHEP 2000, Osaka, Japan. `e-Print Archive: hep-ex/0011044`.
[25] S. Anderson *et al.* (CLEO Collaboration), Conference report CLEO CONF 99-6 (1999).

[26] B. Aubert *et al.* (BaBaR Collaboration), *Phys. Rev.* **D69**, 031101 (2004).
[27] A. Le Yaouanc *et al. Phys. Lett.* **B568**, 254 (2003).
[28] R. Chistov *et al.* (Belle Collaboration), *Phys. Rev. Lett.* **93**, 051803 (2004).
[29] K. Abe *et al.* (Belle Collaboration), Belle-CONF-0439, ICHEP04 8-0685.
[30] E.J. Eichten, K. Lane, C. Quigg, *Phys. Rev. Lett.* **89**, 162002 (2002).
[31] E.S. Swanson, *Phys. Lett.* **B588**, 189 (2004).